

Higgs Boson Mass Bounds in Seesaw Extended Standard Model with Non-Minimal Gravitational Coupling

Bin He^{a1}, Nobuchika Okada^{b2} and Qaisar Shafi^{a3}

^a*Bartol Research Institute, Department of Physics and Astronomy,
University of Delaware, Newark, DE 19716, USA*

^b*Department of Physics and Astronomy, University of Alabama, Tuscaloosa, AL 35487, USA*

Abstract

In the presence of non-minimal gravitational coupling $\xi H^\dagger H \mathcal{R}$ between the standard model (SM) Higgs doublet H and the curvature scalar \mathcal{R} , the effective ultraviolet cutoff scale is given by $\Lambda \approx m_P/\xi$, where m_P is the reduced Planck mass, and $\xi \gtrsim 1$ is a dimensionless coupling constant. In type I and type III seesaw extended SM, which can naturally explain the observed solar and atmospheric neutrino oscillations, we investigate the implications of this non-minimal gravitational coupling for the SM Higgs boson mass bounds based on vacuum stability and perturbativity arguments. A lower bound on the Higgs boson mass close to 120 GeV is realized with type III seesaw and $\xi \sim 10 - 10^3$.

¹ E-mail:hebin@udel.edu

² E-mail:okadan@ua.edu

³ E-mail:shafi@bartol.udel.edu

The search for the SM Higgs boson is arguably the single most important mission of the LHC. According to precision electroweak data and the direct lower mass bound from LEP II, a Higgs boson mass in the range of $114.4 \text{ GeV} \lesssim m_H \lesssim 180 \text{ GeV}$ [1] is favored. If one takes the reduced Planck mass $m_P = 2.4 \times 10^{18} \text{ GeV}$ as a natural cutoff scale of the SM, theoretical considerations based on vacuum stability and perturbativity arguments narrow the SM Higgs boson mass bounds somewhat, namely $128 \text{ GeV} \lesssim m_H \lesssim 175 \text{ GeV}$ [2, 3]. Very recently, it has been reported [4] that the SM Higgs boson mass in the mass range $158 \text{ GeV} \lesssim m_H \lesssim 175 \text{ GeV}$ is excluded at 95% C.L. by the direct searches at the Tevatron.

Clearly, if there exists some new physics beyond the SM between the electroweak scale and the reduced Planck scale, it can affect these theoretical Higgs boson mass bounds. The seesaw mechanism is a simple and promising extension of the SM to incorporate the neutrino masses and mixings observed in solar and atmospheric neutrino oscillations. There are three main seesaw extensions of the SM, type I [5], type II [6], and type III [7], in which new particles, singlet right-handed neutrinos, SU(2) triplet scalar, and SU(2) triplet right-handed neutrinos, respectively, are introduced. These new particles contribute to the renormalization group equations (RGEs) at energies higher than the seesaw scale and as a result, the Higgs boson mass bounds can be significantly altered. The important implications of seesaw models on the Higgs boson mass bounds have been investigated with the reduced Planck mass cutoff for the various seesaw models, type I [8, 9], type II [10] and type III [9].

In general, the non-minimal gravitational coupling between the SM Higgs doublet and the curvature scalar,

$$\xi H^\dagger H \mathcal{R}, \quad (1)$$

can be introduced in the SM. This coupling opens up a very intriguing scenario for inflationary cosmology, namely, the possibility that the SM Higgs field may play the role of inflation field, and this has been investigated in several recent papers [11]-[17]. As pointed out in [18], in the presence of the non-minimal gravitational coupling, it is natural to identify the effective ultraviolet cutoff scale as

$$\Lambda \approx \frac{m_P}{\xi}, \quad (2)$$

for $\xi \gtrsim 1$, rather than m_P . Note that the cutoff may depend on the background field value which in our case is of order the electroweak scale (see last refs. in [11] and [17]).

In this paper, we extend previous work on the Higgs boson mass bounds in type I and III seesaw extended SM [8, 9] to the case with non-minimal gravitational coupling. The ultraviolet cutoff scale is taken to be $\Lambda = m_P/\xi$ in our analysis. We will show that the gravitational

coupling as well as type I and III seesaw effects can dramatically alter the vacuum stability and perturbativity bounds on the SM Higgs boson mass. In particular, the vacuum stability bound on the Higgs boson mass can be lowered to 120 GeV or so, significantly below the usual lower bound of about 128 GeV found in the absence of seesaw and with $\xi = 0$.

In type I seesaw, three generations of SM-singlet right-handed neutrinos $\psi_i (i = 1, 2, 3)$ are introduced. The relevant terms in the Lagrangian are given by

$$\mathcal{L} \supset -y_{ij}\bar{\ell}_i\psi_j H - M_R\bar{\psi}_i^c\psi_i, \quad (3)$$

where ℓ_i is the i -th generation SM lepton doublet. For simplicity, we assume in this paper that the three right-handed neutrinos are degenerate in mass (M_R). At energies below M_R , the heavy right-handed neutrinos are integrated out and the effective dimension five operator is generated by the seesaw mechanism. After electroweak symmetry breaking, the light neutrino mass matrix is obtained as

$$\mathbf{M}_\nu = \frac{v^2}{2M_R}\mathbf{Y}_\nu^T\mathbf{Y}_\nu, \quad (4)$$

where $v = 246$ GeV is the VEV of the Higgs doublet, and $\mathbf{Y}_\nu = y_{ij}$ is a 3×3 Yukawa matrix.

The basic structure of type III seesaw is similar to type I seesaw, except that instead of the singlet right-handed neutrinos, three generations of fermions which transforms as $(\mathbf{3}, 0)$ under the electroweak gauge group $SU(2)_L \times U(1)_Y$ are introduced:

$$\psi_i = \sum_a \frac{\sigma^a}{2} \psi_i^a = \frac{1}{2} \begin{pmatrix} \psi_i^0 & \sqrt{2}\psi_i^+ \\ \sqrt{2}\psi_i^- & -\psi_i^0 \end{pmatrix}. \quad (5)$$

With canonically normalized kinetic terms for the triplet fermions, we replace the SM-singlet right-handed neutrinos of type I seesaw in Eq. (3) by these $SU(2)$ triplet fermions. Assuming degenerate masses (M_R) for the three triplet fermions, the light neutrino mass matrix via type III seesaw mechanism is obtained as

$$\mathbf{M}_\nu = \frac{v^2}{8M_R}\mathbf{Y}_\nu^T\mathbf{Y}_\nu. \quad (6)$$

For a renormalization scale $\mu < M_R$, the heavy fermions are decoupled, and there is no effect on the RGEs for the SM couplings. However, in the presence of the non-minimal gravitational coupling, a factor $s(\mu)$ defined as

$$s(\mu) = \frac{1 + \frac{\xi\mu^2}{m_P^2}}{1 + (6\xi + 1)\frac{\xi\mu^2}{m_P^2}}, \quad (7)$$

is assigned to each term in the RGEs associated with the physical Higgs boson loop corrections [11, 12, 15]. In our analysis, we employ 2-loop RGEs for the SM couplings. Since the SM

beta functions suitably modified with the s -factor are known only at 1-loop level, we employ the beta functions with the s -factor for 1-loop corrections, while the beta functions for 2-loop corrections are without the s -factor. We have checked that the effects of the s -factor in beta functions for 2-loop corrections are negligible as far as our final results are concerned[13].

For the three SM gauge couplings with a renormalization scale $\mu < M_R$, we have

$$\frac{dg_i}{d \ln \mu} = \frac{b_i}{16\pi^2} g_i^3 + \frac{g_i^3}{(16\pi^2)^2} \left(\sum_{j=1}^3 B_{ij} g_j^2 - C_i y_t^2 \right), \quad (8)$$

where g_i ($i = 1, 2, 3$) are the SM gauge couplings,

$$b_i = \left(\frac{81+s}{20}, -\frac{39-s}{12}, -7 \right), \quad B_{ij} = \begin{pmatrix} \frac{199}{50} & \frac{27}{10} & \frac{44}{5} \\ \frac{10}{11} & \frac{35}{6} & 12 \\ \frac{10}{10} & \frac{9}{2} & -26 \end{pmatrix}, \quad C_i = \left(\frac{17}{10}, \frac{3}{2}, 2 \right), \quad (9)$$

and we have included the contribution from the top Yukawa coupling (y_t). We use the top quark pole mass $M_t = 173.1$ GeV and the strong coupling constant at the Z-pole (M_Z) $\alpha_S = 0.1193$ [19]. For the top Yukawa coupling, we have

$$\frac{dy_t}{d \ln \mu} = y_t \left(\frac{1}{16\pi^2} \beta_t^{(1)} + \frac{1}{(16\pi^2)^2} \beta_t^{(2)} \right). \quad (10)$$

Here the one-loop contribution is

$$\beta_t^{(1)} = \left(4 + \frac{s}{2} \right) y_t^2 - \left(\frac{17}{20} g_1^2 + \frac{9}{4} g_2^2 + 8 g_3^2 \right), \quad (11)$$

while the two-loop contribution is given by [20]

$$\begin{aligned} \beta_t^{(2)} = & -12 y_t^4 + \left(\frac{393}{80} g_1^2 + \frac{225}{16} g_2^2 + 36 g_3^2 \right) y_t^2 \\ & + \frac{1187}{600} g_1^4 - \frac{9}{20} g_1^2 g_2^2 + \frac{19}{15} g_1^2 g_3^2 - \frac{23}{4} g_2^4 + 9 g_2^2 g_3^2 - 108 g_3^4 \\ & + \frac{3}{2} \lambda^2 - 6 \lambda y_t^2. \end{aligned} \quad (12)$$

In solving the RGE for the top Yukawa coupling, its value at $\mu = M_t$ is determined from the relation between the pole mass and the running Yukawa coupling [21, 22],

$$M_t \simeq m_t(M_t) \left(1 + \frac{4}{3} \frac{\alpha_3(M_t)}{\pi} + 11 \left(\frac{\alpha_3(M_t)}{\pi} \right)^2 - \left(\frac{m_t(M_t)}{2\pi v} \right)^2 \right), \quad (13)$$

with $y_t(M_t) = \sqrt{2} m_t(M_t)/v$, where $v = 246$ GeV. Here, the second and third terms in parenthesis correspond to one- and two-loop QCD corrections, respectively, while the fourth term comes from the electroweak corrections at one-loop level.

The RGE for the Higgs quartic coupling is given by [20],

$$\frac{d\lambda}{d\ln\mu} = \frac{1}{16\pi^2}\beta_\lambda^{(1)} + \frac{1}{(16\pi^2)^2}\beta_\lambda^{(2)}, \quad (14)$$

with

$$\beta_\lambda^{(1)} = (3 + 9s^2)\lambda^2 - \left(\frac{9}{5}g_1^2 + 9g_2^2\right)\lambda + \frac{9}{4}\left(\frac{3}{25}g_1^4 + \frac{2}{5}g_1^2g_2^2 + g_2^4\right) + 12y_t^2\lambda - 12y_t^4, \quad (15)$$

and

$$\begin{aligned} \beta_\lambda^{(2)} = & -78\lambda^3 + 18\left(\frac{3}{5}g_1^2 + 3g_2^2\right)\lambda^2 - \left(\frac{73}{8}g_2^4 - \frac{117}{20}g_1^2g_2^2 - \frac{1887}{200}g_1^4\right)\lambda - 3\lambda y_t^4 \\ & + \frac{305}{8}g_2^6 - \frac{289}{40}g_1^2g_2^4 - \frac{1677}{200}g_1^4g_2^2 - \frac{3411}{1000}g_1^6 - 64g_3^2y_t^4 - \frac{16}{5}g_1^2y_t^4 - \frac{9}{2}g_2^4y_t^2 \\ & + 10\lambda\left(\frac{17}{20}g_1^2 + \frac{9}{4}g_2^2 + 8g_3^2\right)y_t^2 - \frac{3}{5}g_1^2\left(\frac{57}{10}g_1^2 - 21g_2^2\right)y_t^2 - 72\lambda^2y_t^2 + 60y_t^6. \end{aligned} \quad (16)$$

The Higgs boson pole mass m_H is determined through one-loop effective potential improved by two-loop RGEs. The second derivative of the effective potential at the potential minimum leads to [23]

$$\begin{aligned} m_H^2 = & \lambda\zeta^2v^2 + \frac{3}{64\pi^2}\zeta^2v^2\left\{g_2^4\left(\log\frac{g_2^2\zeta^2v^2}{4\mu^2} + \frac{2}{3}\right)\right. \\ & \left. + \frac{1}{2}\left(g_2^2 + \frac{3}{5}g_1^2\right)^2\left[\log\frac{(g_2^2 + \frac{3}{5}g_1^2)\zeta^2v^2}{4\mu^2} + \frac{2}{3}\right] - 8y_t^4\log\frac{y_t^2\zeta^2v^2}{2\mu^2}\right\}, \end{aligned} \quad (17)$$

where $\zeta = \exp\left(-\int_{M_Z}^\mu \frac{\gamma(\mu)}{\mu}d\mu\right)$, with the anomalous dimension γ of the Higgs doublet evaluated at two-loop level. All running parameters are evaluated at $\mu = m_H$, and the Higgs boson mass is determined as the root of this equation. We have checked that our results on the Higgs boson mass bounds for the SM case ($\xi = 0$ and $M_R \rightarrow \infty$) coincide with the ones obtained in recent analysis [3].

For the renormalization scale $\mu \geq M_R$, the SM RGEs should be modified to include contributions from the singlet and triplet fermions in type I and III seesaw, respectively, so that the RGE evolution of the Higgs quartic coupling is altered. For simplicity, we consider only one-loop corrections from the heavy fermions.

We first consider type I seesaw. For $\mu \geq M_R$, the above RGEs are modified as

$$\begin{aligned} \beta_t^{(1)} & \rightarrow \beta_t^{(1)} + \text{tr}[\mathbf{S}_\nu], \\ \beta_\lambda^{(1)} & \rightarrow \beta_\lambda^{(1)} + 4\text{tr}[\mathbf{S}_\nu]\lambda - 4\text{tr}[\mathbf{S}_\nu^2], \end{aligned} \quad (18)$$

where $\mathbf{S}_\nu = \mathbf{Y}_\nu^\dagger \mathbf{Y}_\nu$, and its corresponding RGE is given by

$$16\pi^2 \frac{d\mathbf{S}_\nu}{d\ln\mu} = \mathbf{S}_\nu \left[6y_t^2 + 2 \operatorname{tr}[\mathbf{S}_\nu] - \left(\frac{9}{10}g_1^2 + \frac{9}{2}g_2^2 \right) + (2+s)\mathbf{S}_\nu \right]. \quad (19)$$

We analyze the RGEs numerically and show how the vacuum stability and perturbativity bounds on Higgs boson mass are altered in the presence of type I seesaw and the non-minimal gravitational coupling. As previously noted, because of the gravitational coupling, we set the ultraviolet cutoff as $\Lambda = m_P/\xi$ for $\xi \geq 1$ ($\Lambda = m_P$ as usual if $\xi < 1$). We define the vacuum stability bound as the lowest Higgs boson mass obtained from the running of the Higgs quartic coupling which satisfies the condition $\lambda(\mu) \geq 0$ for any scale between $m_H \leq \mu \leq \Lambda$. On the other hand, the perturbativity bound is defined as the highest Higgs boson mass obtained from the running of the Higgs quartic coupling with the condition $\lambda(\mu) \leq 4\pi$ for any scale between $m_H \leq \mu \leq \Lambda$.

In order to see the effects of the neutrino Yukawa coupling on the Higgs boson mass bounds, we first examine a toy model with $\mathbf{Y}_\nu = \operatorname{diag}(0, 0, Y_\nu)$. In Figure 1, the vacuum stability and perturbativity bounds on Higgs boson mass as a function of ξ are depicted for various Y_ν values and a fixed seesaw scale $M_R = 10^{13}$ GeV. The results for the perturbativity bound are almost insensitive to Y_ν . On the other hand, for a fixed $\xi < m_P/M_R$, the vacuum instability bound becomes larger, as Y_ν is increased. For a fixed Y_ν , the vacuum instability bound becomes smaller, as ξ is increased. When $\xi > m_P/M_R$ or equivalently $\Lambda < M_R$, the vacuum stability and perturbativity bounds coincides with the SM ones with Λ , as expected. For a fixed cutoff scale $\Lambda > M_R$, the window for the Higgs boson mass between the vacuum stability and perturbative bounds becomes narrower and is eventually closed as Y_ν becomes sufficiently large. This behavior is shown in Figure 2 for various values of ξ . Increasing ξ widens the Higgs mass window for a fixed Y_ν .

It is certainly interesting to consider more realistic cases which are compatible with the current neutrino oscillation data. The light neutrino mass matrix is diagonalized by a mixing matrix U_{MNS} such that

$$\mathbf{M}_\nu = \frac{v^2}{2M_R} \mathbf{S}_\nu = U_{MNS} D_\nu U_{MNS}^T, \quad (20)$$

with $D_\nu = \operatorname{diag}(m_1, m_2, m_3)$, where we have assumed, for simplicity, that the Yukawa matrix \mathbf{Y}_ν is real. We further assume that the mixing matrix has the so-called tri-bimaximal form [24],

$$U_{MNS} = \begin{pmatrix} \sqrt{\frac{2}{3}} & \sqrt{\frac{1}{3}} & 0 \\ -\sqrt{\frac{1}{6}} & \sqrt{\frac{1}{3}} & \sqrt{\frac{1}{2}} \\ -\sqrt{\frac{1}{6}} & \sqrt{\frac{1}{3}} & -\sqrt{\frac{1}{2}} \end{pmatrix}, \quad (21)$$

which is in very good agreement with the current best fit values of the neutrino oscillation data [25]. Let us consider two examples for the light neutrino mass spectrum, the hierarchical case and the inverted-hierarchical case. In the hierarchical case, we have

$$D_\nu \simeq \text{diag}(0, \sqrt{\Delta m_{12}^2}, \sqrt{\Delta m_{23}^2}), \quad (22)$$

while for the inverted-hierarchical case, we choose

$$D_\nu \simeq \text{diag}(\sqrt{-\Delta m_{12}^2 + \Delta m_{23}^2}, \sqrt{\Delta m_{23}^2}, 0). \quad (23)$$

We fix the input values for the solar and atmospheric neutrino oscillation data as [25]

$$\begin{aligned} \Delta m_{12}^2 &= 8.2 \times 10^{-5} \text{ eV}^2, \\ \Delta m_{23}^2 &= 2.4 \times 10^{-3} \text{ eV}^2. \end{aligned} \quad (24)$$

From Eqs. (20)-(24), we can obtain the matrix

$$\mathbf{S}_\nu = \mathbf{Y}_\nu^\dagger \mathbf{Y}_\nu = \mathbf{Y}_\nu^T \mathbf{Y}_\nu = \frac{2M_R}{v^2} U_{MNS} D_\nu U_{MNS}^T. \quad (25)$$

For a given value of M_R , we obtain a concrete 3×3 matrix at the M_R scale, which is used as an input in the RGE analysis. The windows for the Higgs boson pole mass for the hierarchical and inverted-hierarchical cases are shown in Figures 3 and 4, respectively. As M_R or equivalently the Yukawa couplings become large, the window for the Higgs boson mass becomes narrower and is eventually closed for a fixed ξ . In plots for large values of ξ , the Higgs boson mass window first narrows, but opens up again, as M_R is increased. This is because M_R becomes larger than Λ for a sufficiently large ξ .

We next consider type III seesaw. The analysis is analogous to the type I seesaw case. For $\mu \geq M_R$, the RGEs are modified as [9]

$$\begin{aligned} \beta_t^{(1)} &\rightarrow \beta_t^{(1)} + \frac{3}{4} \text{tr} [\mathbf{S}_\nu], \\ \beta_\lambda^{(1)} &\rightarrow \beta_\lambda^{(1)} + 3 \text{tr} [\mathbf{S}_\nu] \lambda - \frac{5}{4} \text{tr} [\mathbf{S}_\nu^2]. \end{aligned} \quad (26)$$

The RGE for \mathbf{S}_ν is given by

$$16\pi^2 \frac{d\mathbf{S}_\nu}{d \ln \mu} = \mathbf{S}_\nu \left[6y_t^2 + \frac{3}{2} \text{tr} [\mathbf{S}_\nu] - \left(\frac{9}{10} g_1^2 + \frac{33}{2} g_2^2 \right) + \frac{3+2s}{4} \mathbf{S}_\nu \right]. \quad (27)$$

In addition, in type III seesaw, the one-loop beta function coefficient of the SM SU(2) gauge coupling is modified as $-(39-s)/12 \rightarrow (9+s)/12$ in the presence of SU(2) triplet fermions.

We first examine the toy model for type III seesaw with $M_R = 10^{13}$ GeV. The results are depicted in Figure 5, which corresponds to Figure 1 for type I seesaw. We can see results similar to those presented in Figure 1. The window for the Higgs boson mass between the vacuum stability and perturbativity bounds is shown in Figure 6 for various ξ values, corresponding to Figure 2 for type I seesaw.

In a more realistic case, we repeat the same analysis as in type I seesaw, except for a factor difference in the definition of the light neutrino mass matrix in type III seesaw, $\mathbf{M}_\nu = \frac{v^2}{8M_R} \mathbf{S}_\nu$. The windows for the Higgs boson pole mass for the hierarchical and inverted-hierarchical cases are shown in Figures 7 and 8, respectively. For large M_R , we can see behavior similar to Figures 3 and 4 for type I seesaw. However, note that for low M_R values, the Higgs boson mass bounds with type III seesaw are different from the SM ones and the range of the Higgs boson mass window is enlarged, as pointed out in [9]. In particular, a relatively light Higgs boson mass close to 120 GeV is now possible. This result can be qualitatively understood in the following way. The presence of the triplet fermions significantly alters the RGE running of the $SU(2)_L$ gauge coupling by making it asymptotically non-free, so that $g_2(\mu)$ for $\mu > M_R$ is larger than the SM value without type III seesaw. In the analysis of the stability bound, the Higgs quartic coupling is small, and the one-loop beta function of the Higgs quartic coupling can be approximated as (see Eq. (15))

$$\beta_\lambda^{(1)} \simeq \frac{1}{16\pi^2} \left[\frac{9}{4} \left(\frac{3}{25} g_1^4 + \frac{2}{5} g_1^2 g_2^2 + g_2^4 \right) - 12y_t^4 \right]. \quad (28)$$

Since the first term on the right hand side is larger in type III seesaw than in the SM case, the Higgs quartic coupling decreases more slowly than in the SM. Consequently, the stability bound on the Higgs boson mass is lowered. For the perturbativity bound, the Higgs quartic coupling is large and the one-loop beta function can be approximated by

$$\beta_\lambda^{(1)} \simeq \frac{1}{16\pi^2} \left[(3 + 9s^2)\lambda^2 - \left(\frac{9}{5} g_1^2 + 9g_2^2 \right) \lambda + 12y_t^2 \lambda - 12y_t^4 \right]. \quad (29)$$

The beta function is smaller than the SM one due to the second term. Therefore, the evolution of the Higgs quartic coupling is slower, and as a result, the Higgs boson mass based on the perturbative bound is somewhat larger than the SM one.

Finally, we note that with type III seesaw, the lower bound on the SM Higgs mass is approximately given by

$$m_H \geq 121.4 \text{ GeV} + 3.0 \text{ GeV} \left(\frac{M_t - 173.1 \text{ GeV}}{1.3 \text{ GeV}} \right) - 2.6 \text{ GeV} \left(\frac{\alpha_S(M_Z) - 0.1193}{0.0028} \right). \quad (30)$$

This is to be compared with a lower bound close to 128 GeV in the absence of type III seesaw.

In conclusion, we have considered the potential impacts of type I and III seesaw on the vacuum stability and perturbativity bounds on the Higgs boson mass in the presence of the non-minimal gravitational coupling, with an effective ultraviolet cutoff scale $\Lambda = m_P/\xi$ for $\xi \geq 1$. For energies higher than the seesaw scale, the heavy fermions introduced in type I and III seesaw are involved in loop corrections and the RGEs of the SM are modified. As a consequence, the vacuum stability and perturbativity bounds on the Higgs boson mass are altered. We have found that for a fixed ξ , as the neutrino Yukawa couplings are increased, the vacuum stability bound grows and eventually merges with the perturbativity bound. Therefore, the Higgs boson mass window is closed at some large Yukawa couplings with a fixed seesaw scale, or some high seesaw scale by fixing the light neutrino mass scale. For a fixed neutrino Yukawa coupling or a fixed seesaw scale, the Higgs boson mass window is enlarged as ξ is increased or equivalently the effective cutoff scale is lowered. A large neutrino Yukawa coupling or equivalently a large seesaw scale affects in similar ways the Higgs mass bounds in both type I and III seesaw. However, with type III seesaw, there is significant lowering of the Higgs mass due to modification of the RGE evolution of the $SU(2)_L$ gauge coupling even if the neutrino Yukawa couplings are negligible. For a low seesaw scale, the Higgs boson mass window between the vacuum stability and perturbative bounds turns out to be wider than the SM one. This is in contrast with type I seesaw where the Higgs boson mass bounds in the SM are reproduced in the small Yukawa coupling limit. We have shown that in type III seesaw, the vacuum stability bound on Higgs mass can be close to the current Higgs mass lower bound of 114.4 GeV [26].

Acknowledgments

We thank Ilia Gogoladze and Mansoor Ur Rehman for useful comments and discussion. This work is supported in part by the DOE Grants, # DE-FG02-91ER40626 (B.H. and Q.S.) and # DE-FG02-10ER41714 (N.O.), and by Bartol Research Institute (B.H.). N.O. would like to thank the Particle Theory Group of the University of Delaware for hospitality during his visit.

References

- [1] C. Amsler *et al.* [Particle Data Group], Phys. Lett. B **667**, 1 (2008).
- [2] N. Cabibbo, L. Maiani, G. Parisi and R. Petronzio, Nucl. Phys. B **158**, 295 (1979); P. Q. Hung, Phys. Rev. Lett. **42**, 873 (1979); M.A.B. Beg, C. Panagiotakopoulos and A. Sirlin, Phys. Rev. Lett. **52** (1984) 883; K. S. Babu and E. Ma, Phys. Rev. Lett. **55**, 3005 (1985); M. Lindner, Z. Phys. C **31**, 295 (1986); M. Sher, Phys. Rept. **179**, 273 (1989);

- G. Altarelli and G. Isidori, Phys. Lett. B **337**, 141 (1994); J. A. Casas, J. R. Espinosa and M. Quiros, Phys. Lett. B **342**, 171 (1995); Phys. Lett. B **382**, 374 (1996); J. R. Espinosa and M. Quiros, Phys. Lett. B **353**, 257 (1995);
- [3] For a recent analysis, see J. Ellis, J. R. Espinosa, G. F. Giudice, A. Hoecker and A. Riotto, Phys. Lett. B **679**, 369 (2009) [arXiv:0906.0954 [hep-ph]]; I. Gogoladze, B. He, and Q. Shafi, Phys. Lett. B **690**, 495 (2010) [arXiv:1004.4217 [hep-ph]].
- [4] [The TEVNPH Working Group of the CDF and D0 Collaborations], arXiv:1007.4587 [hep-ex].
- [5] P. Minkowski, Phys. Lett. B **67**, 421 (1977); T. Yanagida, in *Proceedings of the Workshop on the Unified Theory and the Baryon Number in the Universe* (O. Sawada and A. Sugamoto, eds.), KEK, Tsukuba, Japan, 1979, p. 95; M. Gell-Mann, P. Ramond, and R. Slansky, *Supergravity* (P. van Nieuwenhuizen et al. eds.), North Holland, Amsterdam, 1979, p. 315; S. L. Glashow, *The future of elementary particle physics*, in *Proceedings of the 1979 Cargèse Summer Institute on Quarks and Leptons* (M. Lévy et al. eds.), Plenum Press, New York, 1980, p. 687; R. N. Mohapatra and G. Senjanović, Phys. Rev. Lett. **44**, 912 (1980).
- [6] G. Lazarides, Q. Shafi and C. Wetterich, Nucl. Phys. **B181**, 287 (1981); R. N. Mohapatra and G. Senjanović, Phys. Rev. **D 23**, 165 (1981); M. Magg and C. Wetterich, Phys. Lett. B **94**, 61 (1980); J. Schechter and J. W. F. Valle, Phys. Rev. D **22**, 2227 (1980).
- [7] R. Foot, H. Lew, X. G. He and G. C. Joshi, Z. Phys. C **44**, 441 (1989).
- [8] J. A. Casas, V. Di Clemente, A. Ibarra and M. Quiros, Phys. Rev. D **62**, 053005 (2000).
- [9] I. Gogoladze, N. Okada and Q. Shafi, Phys. Lett. B **668**, 121 (2008).
- [10] I. Gogoladze, N. Okada and Q. Shafi, Phys. Rev. D **78**, 085005 (2008).
- [11] F. L. Bezrukov, arXiv:0810.3165 [hep-ph]; F. L. Bezrukov and M. Shaposhnikov, Phys. Lett. B **659**, 703 (2008) [arXiv:0710.3755 [hep-th]]; F. L. Bezrukov, A. Magnin and M. Shaposhnikov, Phys. Lett. B **675**, 88 (2009) [arXiv:0812.4950 [hep-ph]]; F. Bezrukov, D. Gorbunov and M. Shaposhnikov, JCAP **0906**, 029 (2009) [arXiv:0812.3622 [hep-ph]]; F. Bezrukov and M. Shaposhnikov, JHEP **0907**, 089 (2009) [arXiv:0904.1537 [hep-ph]]; F. Bezrukov, A. Magnin, M. Shaposhnikov and S. Sibiryakov, arXiv:1008.5157 [hep-ph].

- [12] A. O. Barvinsky, A. Y. Kamenshchik and A. A. Starobinsky, JCAP **0811**, 021 (2008) [arXiv:0809.2104 [hep-ph]]; A. O. Barvinsky, A. Y. Kamenshchik, C. Kiefer, A. A. Starobinsky and C. Steinwachs, arXiv:0904.1698 [hep-ph]; A. O. Barvinsky, A. Y. Kamenshchik, C. Kiefer, A. A. Starobinsky and C. F. Steinwachs, arXiv:0910.1041 [hep-ph].
- [13] A. De Simone, M. P. Hertzberg and F. Wilczek, Phys. Lett. B **678**, 1 (2009) [arXiv:0812.4946 [hep-ph]].
- [14] S. C. Park and S. Yamaguchi, JCAP **0808**, 009 (2008) [arXiv:0801.1722 [hep-ph]].
- [15] T. E. Clark, B. Liu, S. T. Love and T. ter Veldhuis, Phys. Rev. D **80**, 075019 (2009) [arXiv:0906.5595 [hep-ph]].
- [16] N. Okada, M. U. Rehman and Q. Shafi, arXiv:0911.5073 [hep-ph].
- [17] M. B. Einhorn and D. R. T. Jones, JHEP **1003**, 026 (2010) [arXiv:0912.2718 [hep-ph]]; S. Ferrara, R. Kallosh, A. Linde, A. Marrani and A. Van Proeyen, arXiv:1004.0712 [hep-th]; arXiv:1008.2942 [hep-th].
- [18] C. P. Burgess, H. M. Lee and M. Trott, JHEP **0909**, 103 (2009); J. L. F. Barbon and J. R. Espinosa, Phys. Rev. D **79**, 081302 (2009); M. P. Hertzberg, arXiv:1002.2995 [hep-ph].
- [19] H. Flacher, M. Goebel, J. Haller, A. Hocker, K. Moenig and J. Stelzer, Eur. Phys. J. C **60**, 543 (2009).
- [20] M. E. Machacek and M. T. Vaughn, Nucl. Phys. B **222**, 83 (1983); Nucl. Phys. B **236**, 221 (1984); Nucl. Phys. B **249**, 70 (1985); C. Ford, I. Jack and D. R. T. Jones, Nucl. Phys. **B387** (1992) 373, [Erratum-ibid. **B504** (1997) 551]; H. Arason, D. J. Castano, B. Keszthelyi, S. Mikaelian, E. J. Piard, P. Ramond and B. D. Wright, Phys. Rev. D **46**, 3945 (1992); V. D. Barger, M. S. Berger and P. Ohmann, Phys. Rev. D **47**, 1093 (1993); M. X. Luo and Y. Xiao, Phys. Rev. Lett. **90**, 011601 (2003).
- [21] See, for example, H. Arason, D. J. Castano, B. Keszthelyi, S. Mikaelian, E. J. Piard, P. Ramond and B. D. Wright, Phys. Rev. D **46**, 3945 (1992); H. E. Haber, R. Hempfling and A. H. Hoang, Z. Phys. C **75**, 539 (1997).
- [22] See, for example, F. Jegerlehner, M. Y. Kalmykov and O. Veretin, Nucl. Phys. B **641**, 285 (2002); Nucl. Phys. B **658**, 49 (2003); F. Jegerlehner and M. Y. Kalmykov, Nucl. Phys. B **676**, 365 (2004).

- [23] J. A. Casas, J. R. Espinosa, M. Quiros and A. Riotto, Nucl. Phys. B **436**, 3 (1995)
[Erratum-ibid. B **439**, 466 (1995)].
- [24] P. F. Harrison, D. H. Perkins, W. G. Scott, Phys. Lett. **B530** 167 (2002).
- [25] B. T. Cleveland *et.al*, Astrophys.J. **496** 505 (1998); Super-Kamiokande Collaboration, Phys. Lett. **B539** 179 (2002); Super-Kamiokande Collaboration, Phys. Rev. **D71** 112005 (2005); M. Maltoni, T. Schwetz, M.A. Tortola, J.W.F. Valle New J.Phys. **6** 122 (2004); A. Bandyopadhyay *et al*, Phys. Lett. **B608** 115 (2005); G. L. Fogli *et al*, Prog. Part. Nucl. Phys. **57** 742 (2006); For a recent review, see, for example, H. Nunokawa, S. J. Parke and J. W. F. Valle, Prog. Part. Nucl. Phys. **60**, 338 (2008).
- [26] R. Barate *et al.*, Phys. Lett. B **565**, 61 (2003).

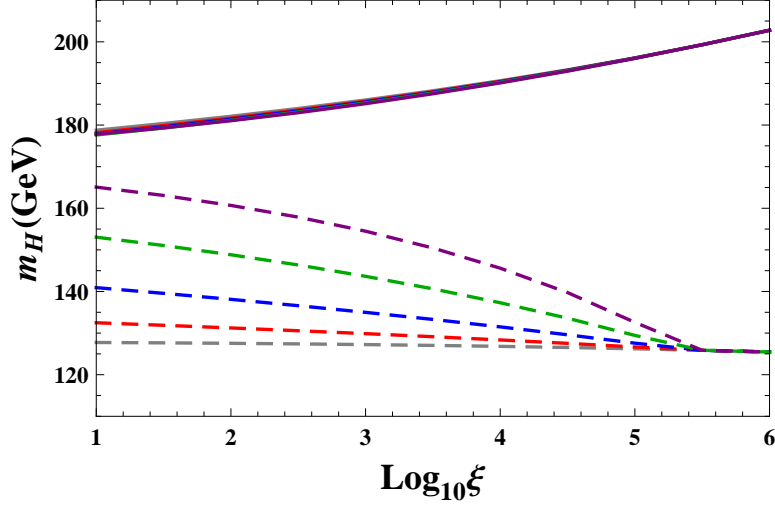


Figure 1: Perturbativity and vacuum stability bounds on Higgs boson mass versus ξ for various Y_ν and $M_R = 10^{13}$ GeV for type I seesaw. The gray lines correspond to $Y_\nu = 0$. The red, blue, green and purple lines correspond to $Y_\nu = 0.6, 0.8, 1.0$ and 1.2 .

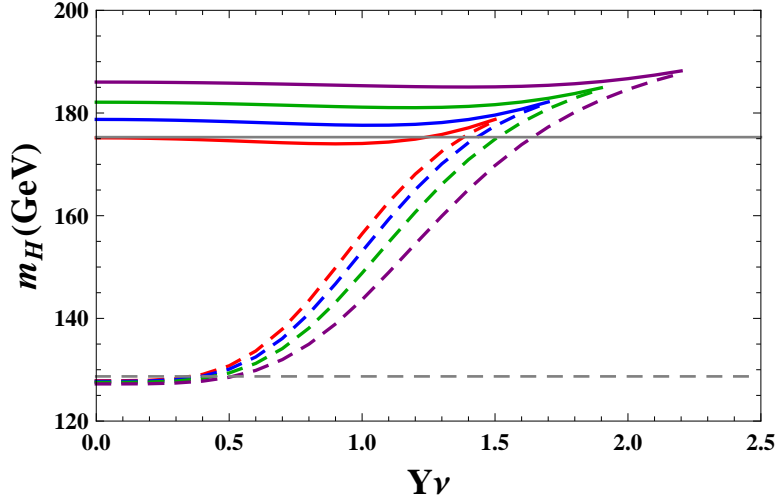


Figure 2: Perturbativity and vacuum stability bounds on Higgs boson mass versus Y_ν for various ξ and $M_R = 10^{13}$ GeV for type I seesaw. The red, blue, green and purple lines correspond to $\xi = 0, 10, 100$ and 10^3 . The gray lines show the bounds in the SM case.

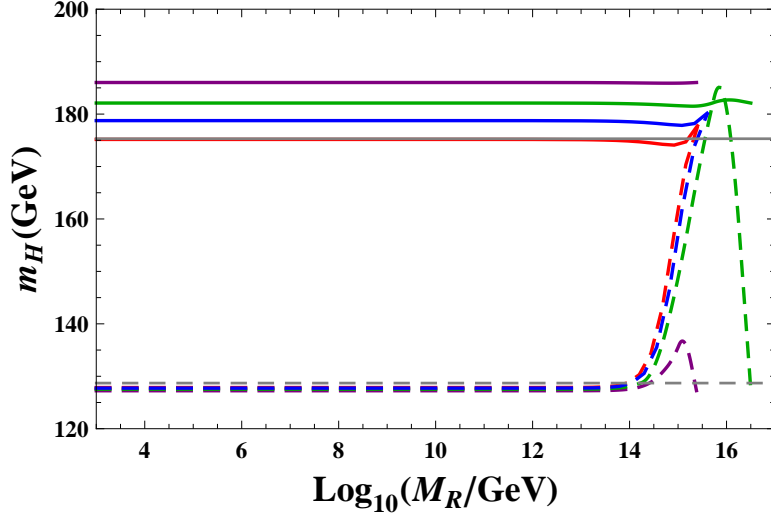


Figure 3: Perturbativity and vacuum stability bounds on Higgs boson mass versus M_R with a hierarchical mass spectrum for type I seesaw. The red, blue, green and purple lines correspond to $\xi = 0, 10, 100$ and 10^3 . The gray lines show the bounds in the SM case.

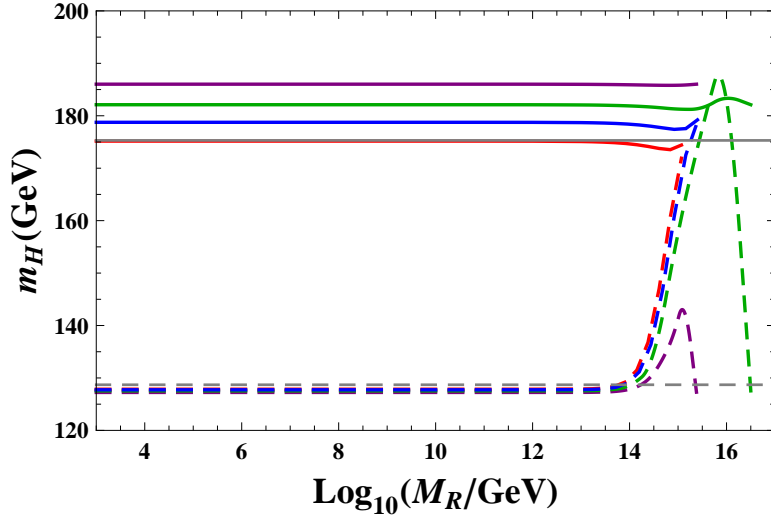


Figure 4: Perturbativity and vacuum stability bounds on Higgs boson mass versus M_R with an inverted hierarchical mass spectrum for type I seesaw. The red, blue, green and purple lines correspond to $\xi = 0, 10, 100$ and 10^3 . The gray lines show the bounds in the SM case.

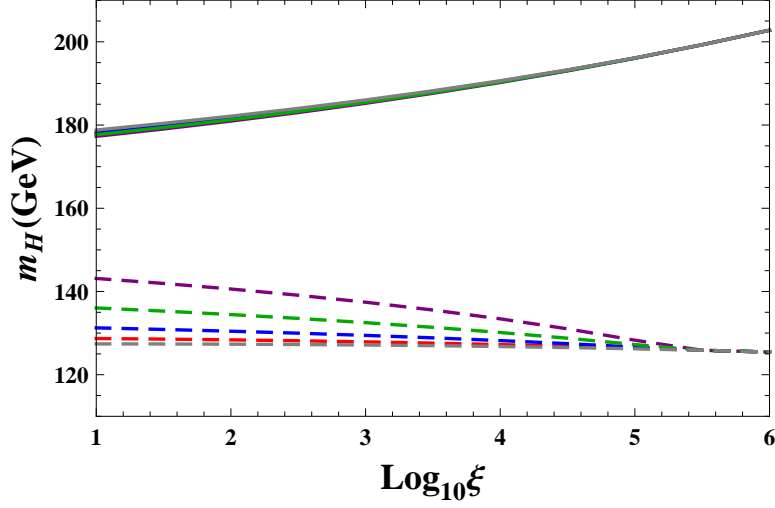


Figure 5: Perturbativity and vacuum stability bounds on Higgs boson mass versus ξ for various Y_ν and $M_R = 10^{13}$ GeV for type III seesaw. The gray lines correspond to $Y_\nu = 0$. The red, blue, green and purple lines correspond to $Y_\nu = 0.6, 0.8, 1.0$ and 1.2 .

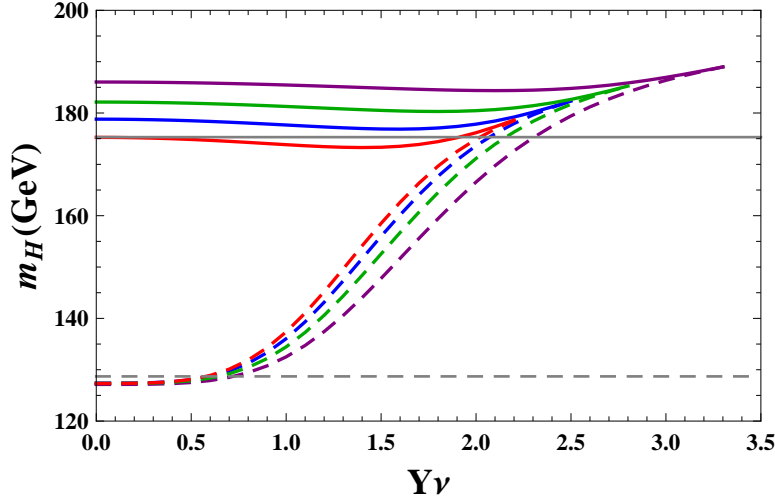


Figure 6: Perturbativity and vacuum stability bounds on Higgs boson mass versus Y_ν for various ξ and $M_R = 10^{13}$ GeV for type III seesaw. The red, blue, green and purple lines correspond to $\xi = 0, 10, 100$ and 10^3 . The gray lines show the bounds in the SM case.

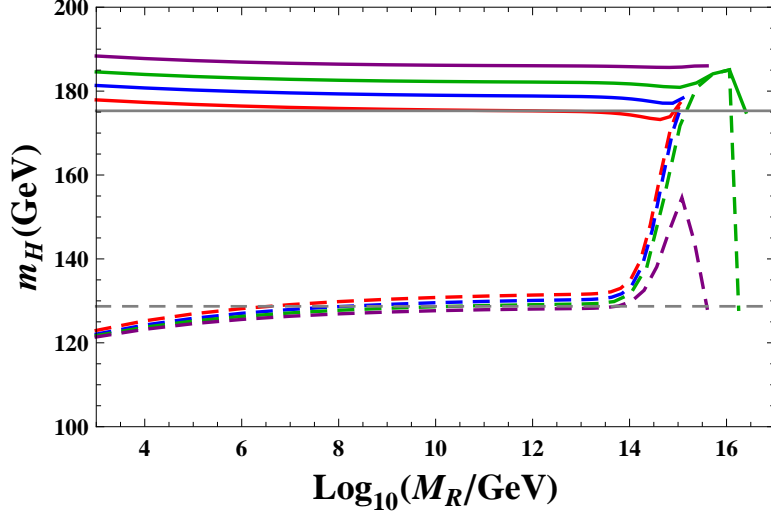


Figure 7: Perturbativity and vacuum stability bounds on Higgs boson mass versus M_R with a hierarchical mass spectrum for type III seesaw. The red, blue, green and purple lines correspond to $\xi = 0, 10, 100$ and 10^3 . The gray lines show the bounds in the SM case.

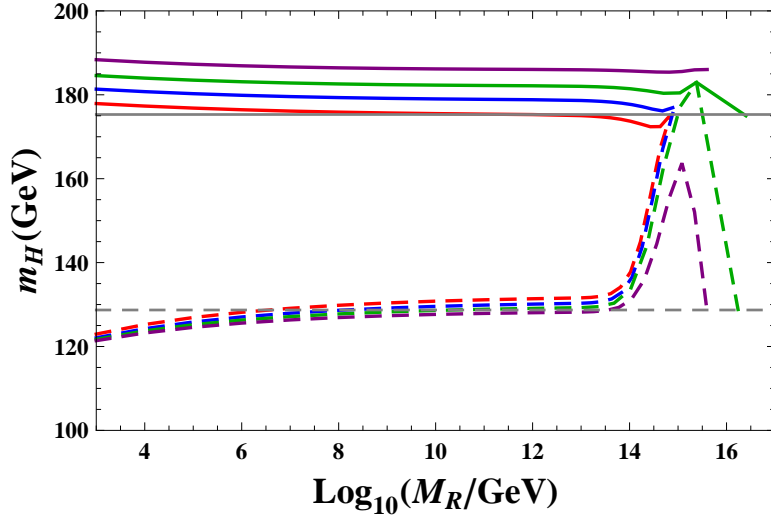


Figure 8: Perturbativity and vacuum stability bounds on Higgs boson mass versus M_R with an inverted hierarchical mass spectrum for type III seesaw. The red, blue, green and purple lines correspond to $\xi = 0, 10, 100$ and 10^3 . The gray lines show the bounds in the SM case.